

HOSTED BY



ELSEVIER

<http://ppr.buaa.edu.cn/>

Propulsion and Power Research

www.sciencedirect.com

ORIGINAL ARTICLE

A mathematical analysis of time dependent flow on a rotating cone in a rheological fluid

S. Saleem^{a,*}, S. Nadeem^b, N. Sandeep^c

^aDepartment of Sciences and Humanities, National University of Computers and Emerging Sciences, Lahore, Pakistan

^bDepartment of Mathematics, Quaid-I-Azam University, 45320, Islamabad 44000, Pakistan

^cFluid Dynamics Division, VIT University, Vellore 632014, India

Received 8 September 2015; accepted 5 January 2016

KEYWORDS

Combined convection;
Rotating cone;
Heat transfer;
Mass transfer;
Jeffrey fluid

Abstract In the present study we have explored the time dependent combined convective flow on a rotating cone in a rotating Jeffrey fluid with the combined effects of heat and mass transfer. The governing equations of motion, energy and mass transfer for unsteady flow are presented and simplified using similar variables. The reduced coupled nonlinear differential equations are solved analytically with the help of strong analytical technique homotopy analysis method. The heat transfer analysis for prescribed wall temperature is considered. Numerical results for Nusselt number and Sherwood number have computed and discussed. The physical features of pertinent parameters are discussed by plotting the graphs of velocity, heat transfer, concentration, skin friction, Nusselt number and Sherwood number.

© 2017 National Laboratory for Aeronautics and Astronautics. Production and hosting by Elsevier B.V.

This is an open access article under the CC BY-NC-ND license

(<http://creativecommons.org/licenses/by-nc-nd/4.0/>).

1. Introduction

Recently, the study of non-Newtonian fluids has found much importance due to their extensive use in many real world applications. Such application include food mixing and chyme movement in the intestine, polymer solutions, paint, flow of plasma, flow of blood, flow of nuclear fuel

slurries, flow of liquid metals and alloys, flow of mercury amalgams and lubrications with heavy oils and greases. In the history of fluid mechanics there is not a single model which exhibits all the properties of non-Newtonian fluids therefore, many mathematical models possessed different physical characteristics exist. However, Jeffrey fluid model is a simple non-Newtonian fluid model which present the relaxation and retardation effects. Some studies on the Jeffrey fluid models are given in the Refs. [1–7].

Mixed convection flow is another important subject which has attracted the attention of various researchers due to its fundamental applications. Solar central receivers exposed to

*Corresponding author. Tel.: +92 3445510959.

E-mail address: salmansaleem_33@hotmail.com (S. Saleem).

Peer review under responsibility of National Laboratory for Aeronautics and Astronautics, China.

<http://dx.doi.org/10.1016/j.jppr.2017.07.003>

2212-540X © 2017 National Laboratory for Aeronautics and Astronautics. Production and hosting by Elsevier B.V. This is an open access article under the CC BY-NC-ND license (<http://creativecommons.org/licenses/by-nc-nd/4.0/>).

Nomenclature

T, C, D	temperature, concentration and mass diffusivity, respectively
C_{fx}, C_{fy}	local skin friction coefficients in the x and y directions, respectively
f, g	dimensionless stream function, velocity components in x - and y -directions, respectively
Gr_1, Gr_2	Grashof numbers due to temperature and concentration distributions, respectively
K, L	thermal conductivity and characteristic length respectively
N	ratio of the Grashof number
Nu_x	local Nusselt number
Pr, Sc	Prandtl and Schmidt numbers respectively
Re_L, Re_x	Reynolds number based on length L and x respectively
Sh_x	local Sherwood number

t, t^*	dimensional and dimensionless times, respectively
u, v, w	velocity components in the x, y and z - directions, respectively
x, y, z	distances measured along meridional section circular section and normal to the cone surface, respectively
α^*	semi-vertical angle of the cone
ξ, ξ^*	volumetric coefficients of the thermal and concentration expansions, respectively
η	similarity variable
θ, ϕ	dimensionless temperature and concentration, respectively
γ_1, γ_2	buoyancy parameters due to the temperature and concentration gradients, respectively
ν, μ	dynamic and kinematic viscosity respectively
ρ	density
A, λ_1	Deborah number and ratio of relaxation to retardation time, respectively.

wind currents, electronic devices cooled by fans, nuclear reactors cooled during emergency shutdown, heat exchangers placed in a low velocity environment are some of the applications of mixed convection flow [8]. The study of convective heat transfer in a rotating flows over a rotating cone is also very important phenomena for the thermal design of various types of equipment's such as rotating heat exchanger, spin stabilized missiles, containers of nuclear waist disposal and geothermal reservoirs. In the existing work, a vertical cone is placed in a non-Newtonian fluid with the axis of the cone being in line with the external flow is explored.

Initially Hering and Grosh [9] have discussed a number of similarity solutions for cones. Himasekhar et al. [10] presented the similarity solution of the mixed convection flow over a vertical rotating cone in a fluid for a wide range of Prandtl numbers. All the above mentioned works refer to steady flows. In many practical problems the flows are unsteady due to the angular velocity of the spinning body which varies with time or due to the free stream angular velocity which varies with time. Ece [11] develops the solution for small time for unsteady boundary layer flow of an impulsively started translating a spinning rotational symmetric body. Roy and Anilkumar [12,13] have investigated the self and semi-similar solutions of an unsteady mixed convection flow over a rotating cone in a rotating viscous fluid.

Boundary layer on a rotating cones, discs and axisymmetric surfaces with a concentrated heat surface has been given by Wang [14]. Mixed convection flow about a cone in a porous medium has been discussed by Yih [15]. Further, Chamkha and Rashad [16] discussed unsteady heat and mass transfer by MHD mixed convection flow from a rotating vertical cone with chemical reaction and solet and dufour Effects.

In general it is challenging to handle nonlinear problems, especially in an analytical way. Perturbation techniques like Variation of iteration method (VIM) and homotopy perturbation method (HPM) [17,18] were frequently used to get solutions of such mathematical investigation. These techniques

are dependent on the small/large constraints, the supposed perturbation quantity. Unfortunately, many nonlinear physical situations in real life do not always have such nature of perturbation parameters. Additional, both of the perturbation techniques themselves cannot give a modest approach in order to adjust or control the region and rate of convergence series. Liao [19] presented an influential analytic technique to solve the nonlinear problems, explicitly the homotopy analysis method (HAM) [17–28]. It offers a suitable approach to control and regulate the convergence region and rate of approximation series, once required.

The objective of the present paper is to discuss the analytical study of unsteady mixed convection flow of a rotating Jeffrey fluid in a rotating cone. The highly nonlinear coupled partial differential equations of Jeffrey fluid model along with heat and mass transfer are simplified by using suitable similarity

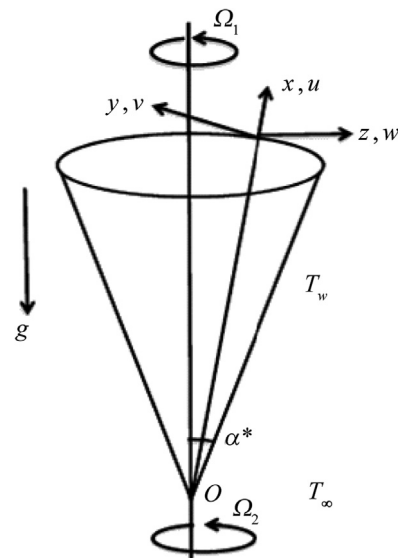


Figure 1 Physical model and coordinate system.

transformations and then solved analytically with the help of analytical technique, homotopy analysis method (HAM). The physical features of pertinent parameters are seen and discussed through various graphs. Final remarks are presented at the last.

2. Mathematical formulation

Let us consider an unsteady non-dissipative incompressible flow of Jeffrey fluid over a rotating cone in a rotating fluid. The time dependent rotation of the cone as well as fluid about the axis of cone is responsible for the unsteadiness in the flow. The system is considered as axisymmetric and fixed. The wall temperature T_w and wall concentration C_w are functions of x . The geometrical model is defined as [Figure 1](#).

In the physical model Ω_1 and Ω_2 are the unsteady rotations, α^* is the angle, u , v and w are velocities along x , y and z -axis, T_w is the wall temperature, q_w is the wall heat flux. The constitutive expressions in a Jeffrey fluid satisfy

$$\mathbf{T} = -\mathbf{PI} + \mathbf{S}.$$

$$\mathbf{S} = \frac{\mu}{1 + \lambda_1} (\dot{\gamma} + \lambda_2 \ddot{\gamma})$$

in which \mathbf{P} denotes the pressure, \mathbf{I} is the identity tensor, μ is the dynamic viscosity, λ_1 is the ratio of relaxation and retardation times, λ_2 is the retardation time,

$$\dot{\gamma} = (\text{grad}\mathbf{V}) + (\text{grad}\mathbf{V})^T$$

$$\ddot{\gamma} = \frac{d}{dt}(\dot{\gamma}),$$

in which \mathbf{V} is the fluid velocity and d/dt is the material derivative. The boundary layer equations of momentum, energy, temperature and concentration for an incompressible Jeffrey fluid in the presence of gravity are

$$x \frac{\partial u}{\partial x} + u + x \frac{\partial w}{\partial z} = 0, \quad (1)$$

$$\begin{aligned} \frac{\partial u}{\partial t} + u \frac{\partial u}{\partial x} + w \frac{\partial u}{\partial z} - \frac{v^2}{x} &= -\frac{v_e^2}{x} + \frac{v}{1 + \lambda_1} \frac{\partial^2 u}{\partial z^2} \\ &+ \frac{v\lambda_2}{1 + \lambda_1} \left\{ u \frac{\partial^3 u}{\partial z^2 \partial x} + \frac{\partial w}{\partial z} \frac{\partial^2 u}{\partial z^2} + \frac{\partial^2 u}{\partial x \partial z} \frac{\partial u}{\partial z} + \right. \\ &\left. w \frac{\partial^3 u}{\partial z^3} + \frac{\partial^3 u}{\partial z^2 \partial t} \right\} \\ &+ g\xi \cos \alpha^* (T - T_\infty) + g\xi^* \cos \alpha^* (C - C_\infty) \end{aligned} \quad (2)$$

$$\begin{aligned} \frac{\partial v}{\partial t} + u \frac{\partial v}{\partial x} + w \frac{\partial v}{\partial z} + \frac{uv}{x} &= \frac{\partial v_e}{\partial t} + \frac{v}{1 + \lambda_1} \frac{\partial^2 v}{\partial z^2} \\ &+ \frac{v\lambda_2}{1 + \lambda_1} \left\{ \frac{\partial^3 v}{\partial z^2 \partial t} + u \frac{\partial^3 v}{\partial z^2 \partial x} + \right. \\ &\left. \frac{\partial u}{\partial z} \frac{\partial^2 v}{\partial x \partial z} + w \frac{\partial^3 v}{\partial z^3} + \frac{\partial w}{\partial z} \frac{\partial^2 v}{\partial z^2} \right\}, \end{aligned} \quad (3)$$

$$\frac{\partial T}{\partial t} + u \frac{\partial T}{\partial x} + w \frac{\partial T}{\partial z} = \alpha \frac{\partial^2 T}{\partial z^2}, \quad (4)$$

$$\frac{\partial C}{\partial t} + u \frac{\partial C}{\partial x} + w \frac{\partial C}{\partial z} = D \frac{\partial^2 C}{\partial z^2}. \quad (5)$$

In the above equations u , v and w are velocity components along x , y and z -axis respectively, T is the temperature, C is the concentration, $g\beta \cos \alpha$ comes due to effects of gravity, k is the thermal diffusivity and D represents mass diffusivity, α^* is the semi-vertical angle of the cone, ν is the kinematic viscosity, ρ is the density, β and β^* are the volumetric co-efficient of expansion for temperature and concentration respectively, C_∞ and T_∞ are the free stream concentration and temperature, v_e is the free stream velocity. The initial conditions and the boundary conditions for this problem are given by Ref. [13].

Defining the following transformations for prescribed wall temperature (PWT) case:

$$\begin{aligned} v_e &= \Omega_2 x \sin \alpha^* (1 - st^*)^{-1}, \\ \eta &= \left(\frac{\Omega \sin \alpha^*}{\nu} \right)^{\frac{1}{2}} (1 - st^*)^{\frac{-1}{2}} z, \\ \alpha_1 &= \frac{\Omega_1}{\Omega} \\ t^* &= (\Omega \sin \alpha^*) t, \\ u(t, x, z) &= -2^{-1} \Omega x \sin \alpha^* (1 - st^*)^{-1} f'(\eta), \\ v(t, x, z) &= \Omega x \sin \alpha^* (1 - st^*)^{-1} g(\eta), \\ w(t, x, z) &= (\nu \Omega \sin \alpha^*)^{\frac{1}{2}} (1 - st^*)^{\frac{-1}{2}} f(\eta), \\ T(t, x, z) - T_\infty &= (T_w - T_\infty) \theta(\eta), \\ (T_w - T_\infty) &= (T_0 - T_\infty) \frac{x}{L} (1 - st^*)^{-2}, \\ C(t, x, z) - C_\infty &= (C_w - C_\infty) \phi(\eta), \\ (C_w - C_\infty) &= (C_0 - C_\infty) \frac{x}{L} (1 - st^*)^{-2}, \\ Gr_1 &= g\beta \cos \alpha^* (T_0 - T_\infty) \frac{L^3}{\nu^2}, \\ Re_L &= \Omega \sin \alpha^* \frac{L^2}{\nu}, \\ \gamma_1 &= \frac{Gr_1}{Re_L^2}, \quad Pr = \frac{\nu}{\alpha}, \quad Sc = \frac{\nu}{D}, \quad N_1 = \frac{\gamma_2}{\gamma_1}, \\ Gr_2 &= g\beta \cos \alpha^* (C_0 - C_\infty) \frac{L^3}{\nu^2}, \quad \gamma_2 = \frac{Gr_2}{Re_L^2}, \\ A &= \lambda_2 \Omega \sin \alpha^* (1 - st^*)^{-1}, \end{aligned} \quad (6)$$

Where γ_1 and γ_2 are the buoyancy parameters, A is the Deborah number. The continuity Eq. (1) is identically satisfied and Eqs. (2) and (5) with boundary conditions for PWT case are

$$\begin{aligned} \frac{1}{1 + \lambda_1} f''' - \left(f + \frac{1}{2} s\eta \right) f'' + \left(\frac{1}{2} f' - s \right) f' - 2(g^2 - (1 - \alpha_1)^2) - 2\gamma_1(\theta + N_1\phi) \\ + \frac{A}{1 + \lambda_1} \left(\frac{1}{2} f' f''' + \frac{1}{2} s\eta f^{iv} - \frac{1}{2} f'^2 + f f^{iv} + 2s f''' \right) = 0 \end{aligned} \quad (7)$$

$$\begin{aligned} \frac{1}{1 + \lambda_1} g'' - (f g' - g f') + s \left(1 - \alpha_1 - g - \frac{1}{2} \eta g' \right) \\ - \frac{A}{1 + \lambda_1} \left(2s g'' + \frac{1}{2} s\eta g''' + \frac{1}{2} g' f' - \frac{1}{2} f'' g + f g''' \right) = 0, \end{aligned} \quad (8)$$

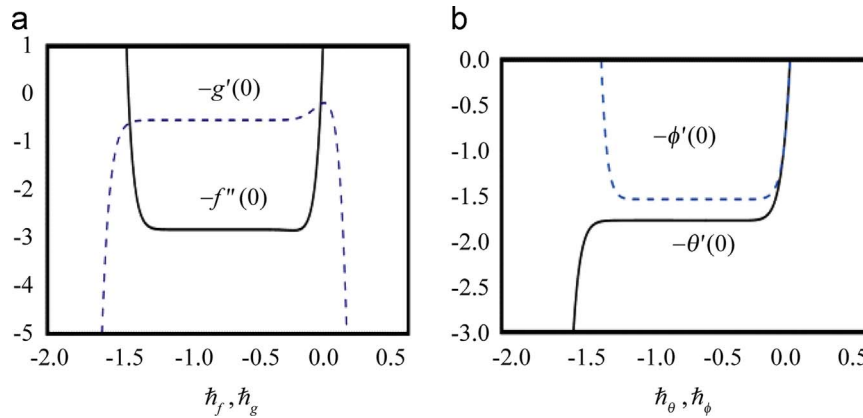


Figure 2 h -curve of $-f''(0)$, $-g'(0)$, $-\theta'(0)$ and $-\phi'(0)$ at 20th approximation (PWT case).

$$\frac{1}{Pr} \theta'' - \left(f \theta' - f' \frac{\theta}{2} \right) - 2s\theta + 2^{-1} s \eta \theta' = 0, \tag{9}$$

$$\frac{1}{Sc} \phi'' - \left(f \phi' - f' \frac{\phi}{2} \right) - 2s\phi + 2^{-1} s \eta \phi' = 0. \tag{10}$$

$$\begin{aligned} f(0) = 0 = f'(0), \quad g(0) = \alpha_1, \quad \theta'(0) = \phi'(0) = -1, \\ f'(\infty) = 0 = f''(\infty), \quad g(\infty) = 1 - \alpha_1, \quad g'(\infty) = 0, \\ \theta(\infty) = \phi(\infty) = 0. \end{aligned} \tag{11}$$

α_1 is the ratio of the angular velocity of the cone and the angular velocity of the fluid. $\alpha_1 = 0$, implies that the fluid is rotating and the cone is at rest, besides the fluid and the cone are rotating with equal angular velocity in the same direction for $\alpha_1 = 0.5$. For $\alpha_1 = 1$, the fluid is at rest and the cone is in rotation. s is the unsteady parameter. The flow is assisting if s is positive and the flow is opposing if s is negative, N is the ratio of the grashof numbers. It has no contribution for chemical diffusion, goes to infinity for the thermal diffusion and shows a positive behavior when the buoyancy forces due to temperature and concentration difference act in the identical pattern and vice versa.

The local skin friction coefficients in tangential and azimuthal directions for the PWT case are, respectively given by

$$C_{fx} = \frac{[2\tau_{xz}]_{z=0}}{\rho [\Omega x \sin \alpha^* (1 - st^*)^{-1}]^2}, \tag{12}$$

$$C_{fy} = \frac{[2\tau_{yz}]_{z=0}}{\rho [\Omega x \sin \alpha^* (1 - st^*)^{-1}]^2}, \tag{13}$$

Where

$$\tau_{xz} = \frac{\mu}{1 + \lambda_1} \left[\frac{\partial u}{\partial z} + \lambda_2 \left(u \frac{\partial^2 u}{\partial x \partial z} + w \frac{\partial^2 u}{\partial z^2} + \frac{\partial^2 u}{\partial t \partial z} \right) \right]_{z=0} \tag{14}$$

$$\tau_{yz} = \frac{\mu}{1 + \lambda_1} \left[\frac{\partial v}{\partial z} + \lambda_2 \left(u \frac{\partial^2 v}{\partial x \partial z} + w \frac{\partial^2 v}{\partial z^2} + \frac{\partial^2 v}{\partial t \partial z} \right) \right]_{z=0} \tag{15}$$

Invoking Eqs. (14) and (15) into Eqs. (12) and (13) and then non-dimensionlizing, we obtain

Table 1 Convergence of HAM solution for different order of approximations.

Order of convergence	$-f''(0)$	$-g'(0)$	$-\theta'(0)$	$-\phi'(0)$
1	2.768	0.264	1.6444	1.53333
5	2.82153	0.5467	1.76784	1.53577
10	2.82719	0.5417	1.76802	1.53565
12	2.82654	0.5413	1.7679	1.53556
15	2.82656	0.5411	1.7679	1.53556
20	2.82644	0.5410	1.76789	1.53556
25	2.82644	0.5410	1.76789	1.53556

$$C_{fx} Re_x^{\frac{1}{2}} = \frac{1}{1 + \lambda_1} \left[-f'' + \frac{A}{2} (f'f'' - 3sf'' + 2ff''' + \eta sf''') \right]_{\eta=0},$$

$$C_{fy} Re_x^{\frac{1}{2}} = \frac{1}{1 + \lambda_1} \left[-g' - \frac{A}{2} (3sg' - f'g' + 2g''f + s\eta g'') \right]_{\eta=0}. \tag{16}$$

The local Nusselt number and local Sherwood number for the PWT case are as follow

$$\begin{aligned} Nu_x Re_x^{-\frac{1}{2}} &= -\theta'(0), \\ Sh_x Re_x^{-\frac{1}{2}} &= -\phi'(0). \end{aligned} \tag{17}$$

Where $Re_x = \frac{x^2 \Omega \sin \alpha^* (1 - st^*)^{-1}}{\nu}$ is the Reynolds number.

3. Homotopy analysis method

Eqs. (7)–(11) are solved by using homotopy analysis method (HAM). This method was developed by Shijun Liao in 1992. It is always valid no matter, whether there exist small physical parameters or not (a requirement for perturbation techniques). It is applicable for both weakly as well as strongly nonlinear problems. It provides great choice to select the base functions of solutions and flexibility in determining the linear operators. Also it offers a convenient way to guarantee the convergence of series solutions. In this way HAM distinguishes itself from other analytical techniques such as Adomain decomposition

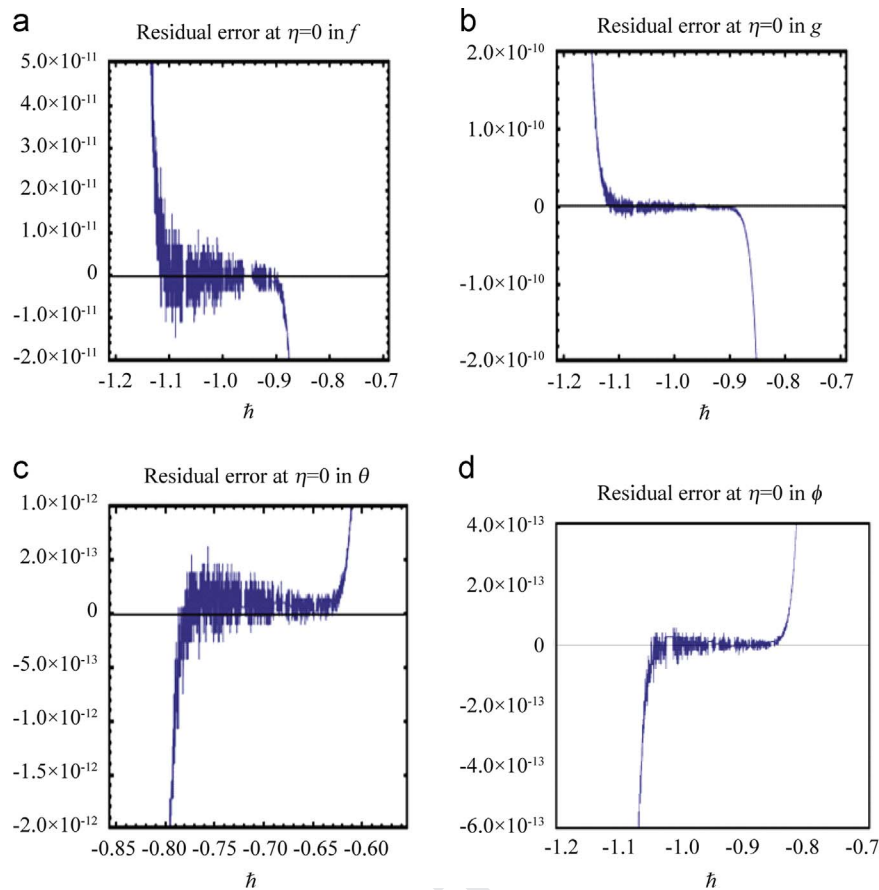


Figure 3 Residual errors for velocities, temperature and concentration, respectively.

method, delta expansion method. Some studies on the method are presented in Refs. [15–23].

We have chosen the following initial guesses and linear operators respectively:

$$f_0(\eta) = 0 \quad (18)$$

$$g_0(\eta) = \exp(-\eta) \quad (19)$$

$$\theta_0(\eta) = \exp(-\eta) \quad (20)$$

$$\phi_0(\eta) = \exp(-\eta) \quad (21)$$

The auxiliary linear operators are

$$\zeta_f(\eta) = f'''' - f' \quad (22)$$

$$\zeta_g(\eta) = g'' - g \quad (23)$$

$$\zeta_\theta(\eta) = \theta'' - \theta \quad (24)$$

$$\zeta_\phi(\eta) = \phi'' - \phi \quad (25)$$

To avoid the repetition just discussion is presented in the coming section.

4. Convergence of the analytical solutions

Obviously the series solutions obtained by homotopy analysis method contain the convergence control parameter \hbar .

This parameter controls the convergence region and the rate of approximation of the HAM solution. As pointed out by Liao [17] to ensure the convergence of the solutions in the admissible range of the values of the auxiliary parameters $\hbar_f, \hbar_g, \hbar_\theta$ and \hbar_ϕ , one can draw the \hbar -curve for 20th order approximations. It is evident from Figure 2(a) and (b) that the admissible range of values of $\hbar_f, \hbar_g, \hbar_\theta$ and \hbar_ϕ are $-1.2 \leq \hbar_f \leq -0.3, -1.3 \leq \hbar_g \leq -0.4, -1.4 \leq \hbar_\theta \leq -0.3, -1.1 \leq \hbar_\phi \leq -0.3$. The convergence Table 1 is prepared for each of the function up to 25th order of approximations. Residual errors for velocity, temperature and concentration are also shown in Figure 3(a), (b), (c) and (d).

5. Results and discussion

The main purpose of this section is to present the solutions of the governing problem. For this the results for PWT case are presented in Figures 4 to 9. Comparison of present results with previous available results [13] is presented in Table 2. The variation of Nusselt number and Sherwood number for different parameters is computed in Table 3. The influences of ratio of angular velocities α_1 , ratio of the relaxation to the retardation time λ_1 , buoyancy parameter γ_1 and Deborah number A on tangential velocity $-f'(\eta)$ are plotted in Figure 4(a)–(d), respectively. It is observed that

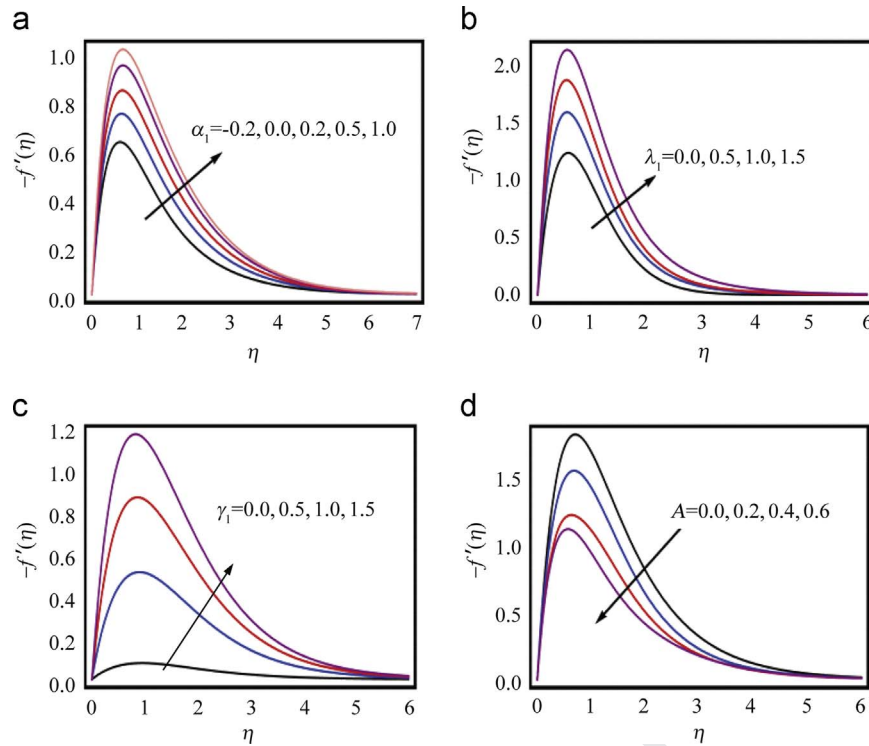


Figure 4 (a) Influence of α_1 on $-f'$, (b) influence of λ_1 on $-f'$, (c) influence of γ_1 on $-f'$, and (d) influence of A on $-f'$.

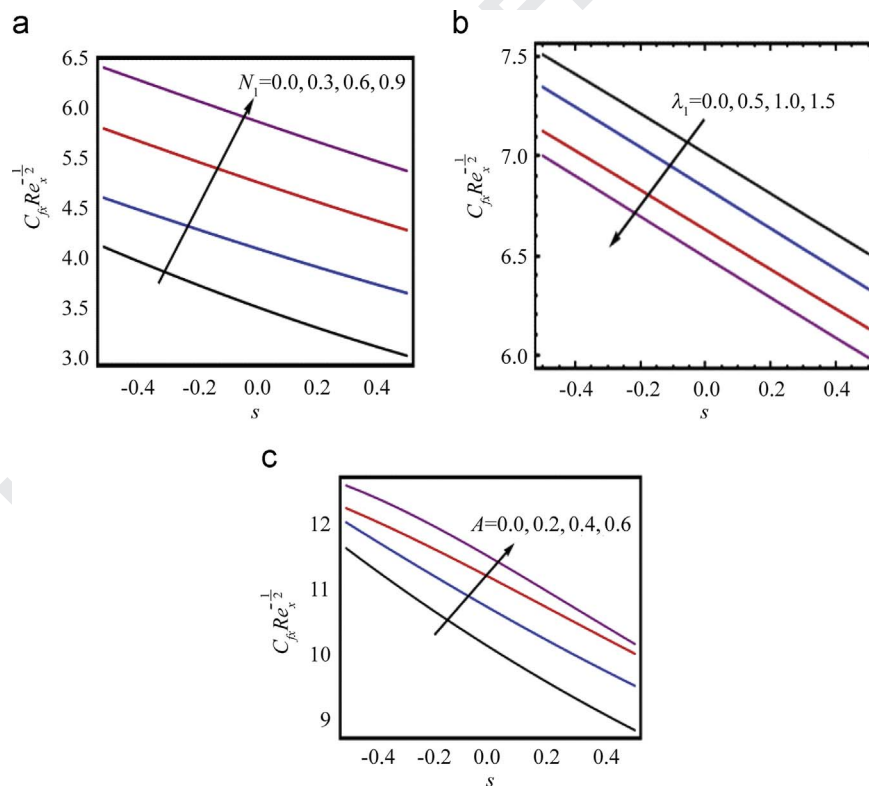


Figure 5 (a) Influence of N_1 on $-f''(0)$, (b) influence of λ_1 on $-f''(0)$, and (c) influence of A on $-f''(0)$.

tangential velocity decreases for A while it increases for all other parameters. It is established from Figure 4(a) that when $\gamma = 0.5$ the fluid and the cone are in rotation with compatible angular velocity in the similar direction and

the flow is only due to the favorable pressure gradient i.e. $\gamma_1 = 1$. For $\alpha_1 > 0.5$, the magnitude of velocity $-f'(\eta)$ increases on the other hand the variation reduces for $\alpha_1 < 0.5$. It is found that for $\alpha_1 < 0$ the velocity field

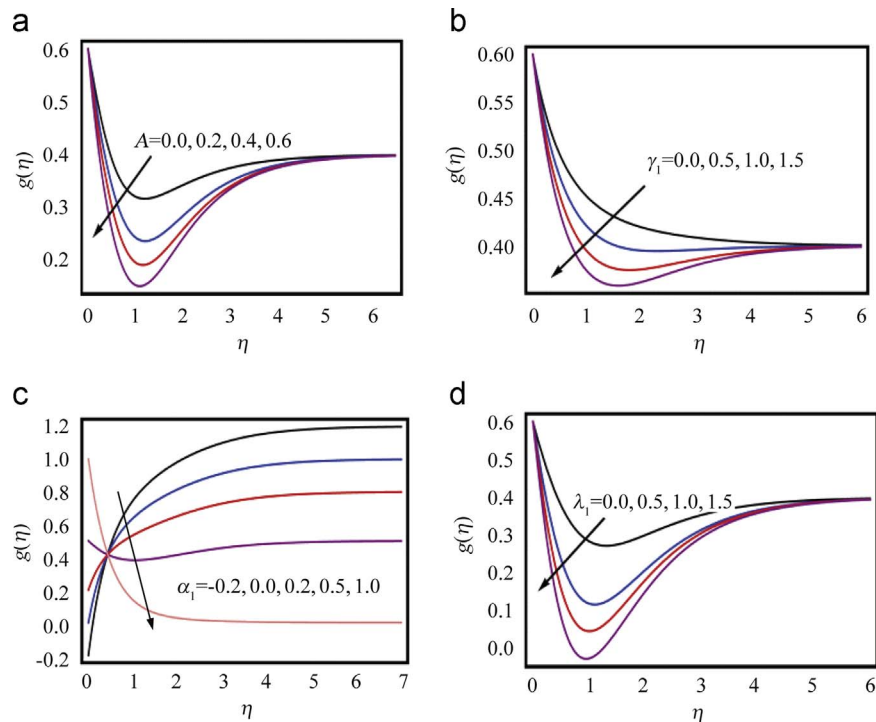


Figure 6 (a) Influence of A on g , (b) influence of α_1 on g , (c) influence of γ_1 on g , and (d) influence of λ_1 on g .

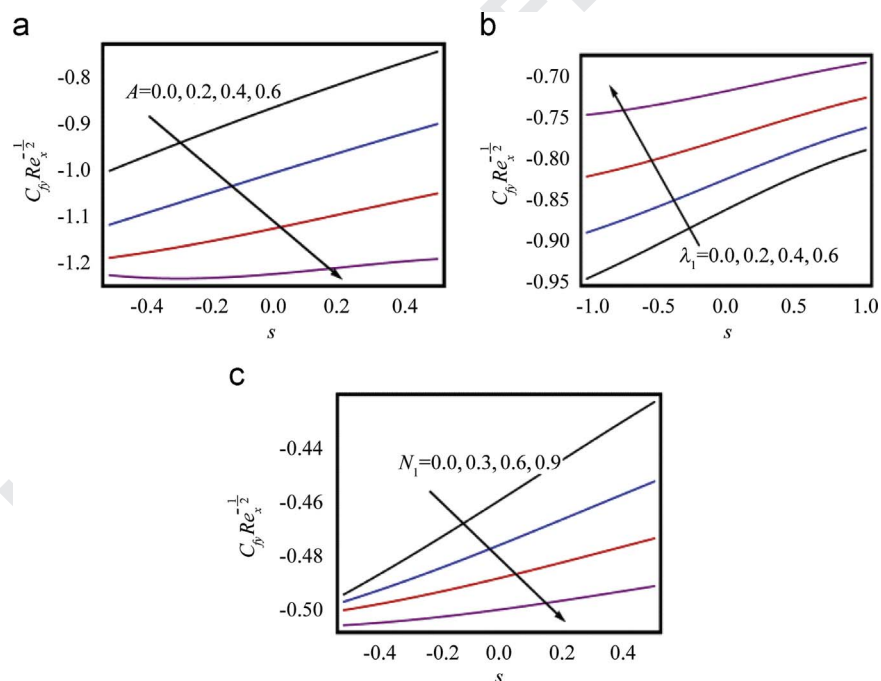


Figure 7 (a) Influence of A on $-g'(0)$, (b) influence of λ_1 on $-g'(0)$, and (c) influence of N_1 on $-g'(0)$.

$-f'(\eta)$ reaches asymptotically at the edge of the boundary layer in an oscillatory style. Actually such oscillations occur due to the surplus convection of angular momentum seems in the region of boundary layer.

In Figure 5(a)–(c) the variation of ratio of the buoyancy forces N_1 , Deborah number A and ratio of the

relaxation to the retardation time λ_1 on tangential skin friction coefficient has been discussed. It is depicted from the Figure 5(a) and (b), that tangential skin friction coefficient increases by increasing N_1 and A respectively. Physically, we can say that near the boundaries of cone the temperature of the wall is greater than the temperature

of the fluid which ultimately increases the Gr_2 as compared to Gr_1 , thus larger N_1 gives the larger skin friction values. It is found that tangential skin friction coefficient decreases as λ_1 increases (see Figure 5(c)).

Figure 6(a)–(d) are devoted to see the variation of Deborah number A , ratio of angular velocities α_1 , buoyancy parameter γ_1 and ratio of the relaxation to the retardation time λ_1 on azimuthal velocity $g(\eta)$, respectively. The behavior of A , α_1 , γ_1 and λ_1 on azimuthal velocity $g(\eta)$ are opposite to that of tangential velocity $-f'(\eta)$. It is observed from Figure 7(a)–(c) that with the increase in A and N_1 , azimuthal skin friction coefficients increases, but the behavior is opposite for λ_1 . Since the effects of Pr and Sc on the velocity profiles in tangential and azimuthal

directions are comparatively small, the profiles are therefore neglected.

Here Figure 8 is displayed for different values Pr on temperature field θ . It is indicated that thermal boundary layer thickness decreases for increasing values of Pr . This is due to the fact that higher Prandtl number fluid has a lower thermal conductivity which results in thinner thermal boundary layer. The concentration profile ϕ is predicted to decrease with increase in the values of Sc as shown in Figure 9.

It is depicted that our series solutions are in good agreement with the numerical results reported by Anilkumar [13] for viscous fluid (see Table 2). Table 3 presents the numerical values of Nusselt number $-\theta'(0)$ and Sherwood number $-\phi'(0)$ for various values of A , λ_1 , Pr and Sc respectively. From the Table 3 it is clear that the Nusselt number increases by increasing λ_1 and Pr and decreasing by an increase in A and Sc . Further we noted that the Sherwood number is a decreasing function of A , Pr and Sc but increases with an increase in λ_1 .

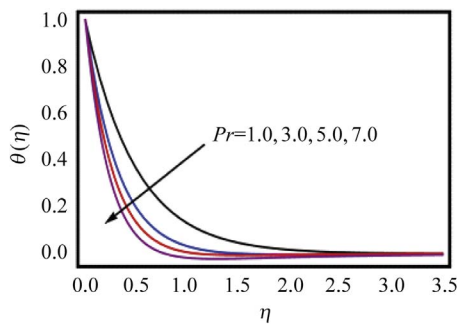


Figure 8 Influence of Pr on θ .

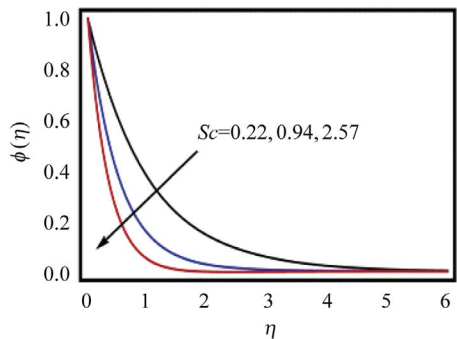


Figure 9 Influence of Sc on ϕ .

Table 3 Values of Nusselt number and Sherwood number for different parameters.

A	λ_1	Pr	Sc	$-\theta'(0)$	$-\phi'(0)$
0	0.1	0.7	0.8	0.98151	1.04188
0.3				0.96159	1.0226
0.6				0.94601	1.00705
0.9				0.93327	0.99430
0.1	0			0.95890	1.01926
	0.2			0.97211	1.03322
	0.4			0.98289	1.04459
	0.6			0.99176	1.05394
		0.4		0.96984	1.28445
		0.8		1.26921	1.26374
		1.2		1.50904	1.25355
		1.6		1.69413	1.24753
			0.4	1.30587	1.23219
			0.8	1.26921	1.19703
			1.2	1.25023	1.17877
			1.6	1.23869	1.16766

Table 2 Comparison of the results $(-f''(0), -g'(0), -\theta'(0), -\phi'(0))$ with those of Anilkumar [13].

λ_1	α_1	HAM				Numerical [13]			
		$-f''(0)$	$-g'(0)$	$-\theta'(0)$	$-\phi'(0)$	$-f''(0)$	$-g'(0)$	$-\theta'(0)$	$-\phi'(0)$
1.0	0.0	0.63243	-0.63948	0.81920	0.95066	0.63241	-0.63949	0.81922	0.95065
	0.25	1.31337	-0.22764	0.89010	1.02811	1.31339	-0.22765	0.89011	1.02812
	0.50	1.84795	0.19805	0.93706	1.07977	1.84798	0.19806	0.93700	1.07977
	0.75	2.24658	0.62679	0.96560	0.11130	2.24659	0.62679	0.96563	0.11132
3.0	0.0	3.79524	-0.59651	1.02862	1.18645	3.79522	-0.59651	1.02869	1.18645
	0.25	4.31853	-0.13694	1.06525	1.22640	4.31854	-0.13691	1.06539	1.22639
	0.50	4.73959	0.33554	1.09111	1.25442	4.73958	0.33552	1.09111	1.25444
	0.75	5.05950	0.81200	1.10711	1.27224	5.05951	0.81201	1.10712	1.27223

6. Conclusions

Unsteady mixed convection flow on a rotating cone in a rotating non-Newtonian fluid has been investigated. Homotopy analysis method is employed for the solutions of the governing ordinary differential equations. The newly calculated results are acknowledged to be in conventional agreement with the formerly published results accessible in the literature. The acquired results have promising applications in engineering and will now be available for experimental verification to give confidence for the well-posedness of this nonlinear boundary value problem. The main points of the above study are as follow.

- The behavior of α_1 , γ_1 , A and λ_1 on velocities ($-f'(\eta)$, $g(\eta)$) are opposite.
- The effects of Pr is to reduces the thermal boundary layer.
- The influence of Sc is to decrease the concentration field ϕ .
- The local skin friction coefficients is an increasing function of N_1 , A and γ_1 .

References

- [1] S. Nadeem, A. Hussain, M. Khan, Stagnation flow of a jeffrey fluid over a shrinking sheet, *Z. Naturforsch* 65a (2010) 540–548.
- [2] T. Chinyoka, O.D. Makinde, Analysis of non-Newtonian flow with reacting species in a channel filled with a saturated porous medium, *J. Petrol. Sci. Engg.* 121 (2014) 1–8.
- [3] T. Hussain, S.A. Shehzad, T. Hayat, A. Alsaedi, F. Al-Solamy, M. Ramzan, Radiative hydromagnetic flow of jeffrey nanofluid by an exponentially stretching sheet, *PLoS One.* 9 (8) (2014) e103719.
- [4] M. Qasim, Heat and mass transfer in a Jeffrey fluid over a stretching sheet with heat source/sink, *Alex. Eng. J.* 52 (4) (2013) 571.
- [5] M. Turkyilmazoglu, I. Pop, Exact analytical solutions for the flow and heat transfer near the stagnation point on a stretching/shrinking sheet in a Jeffrey fluid, *Int. J. Heat. Mass Transf.* 57 (2013) 82–88.
- [6] S.A. Shehzad, T. Hussain, T. Hayat, M. Ramzan, A. Alsaedi, Boundary layer flow of third grade nanofluid with Newtonian heating and viscous dissipation, *J. Cent. South Univ.* 22 (1) (2015) 360–367.
- [7] T. Hayat, S.A. Shehzad, M. Qasim, S. Obaidat, Radiative flow of Jeffery fluid in a porous medium with power law heat flux and heat source, *Nucl. Eng. Des.* 243 (2012) 15–19.
- [8] D. Li, F. Labropulu, I. Pop, Mixed convection flow of a viscoelastic fluid near the orthogonal stagnation point on a vertical surface, *Int. J. Therm. Sci.* 50 (2011) 1698–1705.
- [9] R.G. Hering, R.J. Grosh, Laminar combined convection from a rotating cone, *ASME J. Heat. Transf.* 85 (1963) 29–34.
- [10] K. Himasekhar, P.K. Sarma, K. Janardhan, Laminar mixed convection from a vertical rotating cone, *Int. Comm. Heat. Mass Transf.* 16 (1989) 99–106.
- [11] M.C. Ece, The initial boundary-layer flow past a translating and spinning rotational symmetric body, *J. Eng. Math.* 26 (1992) 415–428.
- [12] D. Anilkumar, S. Roy, Unsteady mixed convection from a rotating cone in a rotating fluid due to the combined effects of thermal and mass diffusion, *Int. J. Heat. Mass Transf.* 47 (2004) 1673–1684.
- [13] D. Anilkumar, S. Roy, Unsteady mixed convection flow on a rotating cone in a rotating fluid, *Appl. Math. Comput.* 155 (2004) 545–561.
- [14] C.Y. Wang, Boundary layers on rotating cones, discs and axisymmetric surfaces with a concentrated heat source, *Acta Mech.* 81 (1990) 245–251.
- [15] K.A. Yih, Mixed convection about a cone in a porous medium: the entire regime, *Int. Commun. Heat. Mass Transf.* 26 (1999) 1041–1050.
- [16] A.J. Chamkha, A.M. Rashad, Unsteady heat and mass transfer by MHD mixed convection flow from a rotating vertical cone with chemical reaction and sores and dufour effects, *Can. J. Chem. Eng.* 92 (2014) 758–767.
- [17] S.J. Liao, *Beyond Perturbation: Introduction to the Homotopy Analysis Method*, Chapman & Hall/CRC Press, Boca Raton, 2003.
- [18] S.J. Liao, Notes on the homotopy analysis method: some definitions and theorems, *Commun. Nonlinear Sci. Numer. Simul.* 14 (2009) 983–997.
- [19] M.M. Rashidi, A.M. Siddiqui, M. Asadi, Application of homotopy analysis method to the unsteady squeezing flow of a second grade fluid between circular plates, *Mathematical Problems in Engineering*, 2010.
- [20] R. Ellahi, A. Riaz, Analytical solutions for MHD flow in a third-grade fluid with variable viscosity, *Math. Comput. Modell.* 52 (2010) 1783–1793.
- [21] R. Ellahi, S. Afzal, Effects of variable viscosity in a third grade fluid with porous medium: an analytic solution, *Commun. Nonlinear Sci. Numer. Simul.* 14 (2009) 2056–2072.
- [22] M.M. Rashidi, M.T. Rastegari, M. Asadi, O. Anwar Bég, A study of non-newtonian flow and heat transfer over a non-isothermal wedge using the homotopy analysis method, *Chem. Eng. Comm.* 199 (2012) 231–256.
- [23] S. Abbasbandy, Homotopy analysis method for heat radiation equation, *Int. Comm. Heat. Mass Transf.* 34 (2007) 380–387.
- [24] S. Nadeem, S. Saleem, Analytical treatment of unsteady mixed convection MHD flow on a rotating cone in a rotating frame, *J. Taiwan Inst. Chem. Eng.* 44 (2013) 596–604.
- [25] M.M. Rashidi, M. Keimaneh, S.C. Rajvanshi, Study of pulsatile flow in a porous annulus with the homotopy analysis method, *Int. J. Numer. Methods Heat Fluid Flow* 22 (8) (2012) 971–989.
- [26] N. Sandeep, A.V.B. Reddy, V. Sugunamma, Effect of radiation and chemical reaction on transient MHD free convective flow over a vertical plate through porous media, *Chem. Process Eng. Res.* 2 (2012) 1–9.
- [27] S. Nadeem, S. Saleem, Unsteady mixed convection flow of nanofluid on a rotating cone with magnetic field, *Appl. Nanosci.* 4 (2013) 405–414.
- [28] H.N. Hassan, M.M. Rashidi, Analytical solution for three-dimensional steady flow of condensation film on inclined rotating disk by optimal homotopy analysis method, *Walailak. J. Sci. Tech. & Tech.* 10 (5) (2013) 479–498.